Investigation of systematic errors in GRACE temporal gravity field solutions using the improved energy balance approach (EGU2020-11504)

Metehan Uz[1] (uzme16@itu.edu.tr) Orhan Akyılmaz[1] Jürgen Kusche[2] C.K. Shum[3,5] Aydın Üstün[4] Yu Zhang [3]

1 Geomatics Department, Graduate School of Science Engineering and Technology, Istanbul Technical University, Istanbul, Turkey
2 Institute of Geodesy and Geoinformation, Bonn University, Bonn, Germany
3 Department of Geodetic Science, School of Earth Sciences, The Ohio State University,Columbus, OH, USA
4 Department of Geomatics, Faculty of Engineering, Kocaeli University, Kocaeli, Turkey
5 Institute of Geodesy and Geophysics, Chinese Academy of Sciences, China

Abstract

In this study, we investigate systematic errors in our temporal gravity solutions computed using the improved energy balance approach (EBA) (Shang et al. 2015) by reprocessing the GRACE JPL RL03 L1B data product. Our processing consists of two steps: the first part is the estimation of in-situ geopotential differences (GPD) at the satellite altitude using the energy balance formalism, the second part is the estimation of spherical harmonic coefficients (SHCs) of the global temporal gravity field model using the estimated GPDs. The first step includes daily dynamic orbit reconstruction by readjusting the reduced-dynamic (GNV1B) orbit considering the reference model, and estimating the accelerometer calibration parameters. This is coupled with the alignment of the inter-satellite velocity pitch from KBR range rate observations. Due to the strategy of using KBR range-rate in our processing algorithm, the estimation of in-situ geopotential differences (GPD) includes both the systematic errors and the high-frequency noise that result from the range-rate observations. Since estimated GPDs are linearly connected with the spherical harmonic coefficients (SHCs) of the global gravity field model, our temporal models are affected by these errors, especially in high-degree coefficients of the temporal gravity field solutions (from n=25 to n=60).

In order to increase our solution accuracy, we fit additional empirical parameters for different arc lengths to mitigate the systematic errors in our GPD estimates, thus improving our temporal gravity field solutions. Our EBA approach GRACE monthly gravity field models are validated by comparisons to the official L2 data products, including the official solutions from CSR [Bettadpur, 2018] and also ITSG-Grace2018 [Mayer-Gürr et al., 2018, Kvas et al., 2019].

A. Systematic Errors in Temporal Models

- We investigate systematic errors in our temporal gravity solutions computed using the improved energy balance approach (EBA) [Guo et al., 2015, Shang et al., 2015] by reprocessing the GRACE JPL RL03 L1B data product [GRACE,] as well as the Atmospheric-Oceanic Dealiasing (AOD1B) RL06 model [Dobslaw et al., 2017].

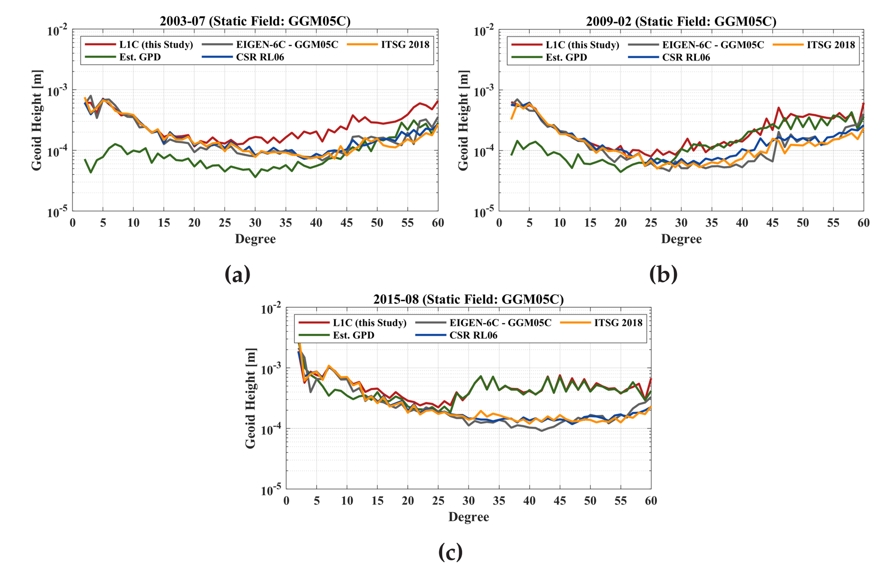

Figure 1: The degree variance of the temporal models of this study, CSR RL06 [Bettadpur, 2018], and ITSG-Grace2018 [Mayer-Gürr et al., 2018, Kvas et al., 2019] for 2003-07 (a), 2009-02 (b) and 2015-08 (c) in terms of geoid undulations, respectively

- The "Improved" EBA reformulates the potential rotation term including the time-variable part of the gravitational potential and expressed with the following new formula

The former energy eqution [Jekeli, 1999]

$$V_{12} = \vec{\dot{x}}_1^T \vec{\dot{x}}_{12} + \frac{1}{2}|\vec{\dot{x}}_{12}|^2 - \sum_k \int_{t_0}^{t} (\overline{F}_{2_k}\dot{x}_{2_k} - \overline{F}_{1_k}\dot{x}_{1_k})dt + \int_{t_0}^{t} \frac{\partial V}{\partial t}dt - E_{0_{12}}$$

$$\int_{t_0}^{t} \frac{\partial V_{12}}{\partial t}dt \approx -\omega_e(x_{12_1}\dot{x}_{2_2} - x_{2_2}\dot{x}_{12_1} - x_{1_1}\vec{\dot{x}}_{12_2} + x_{12_2}x_{1_1})$$

$$\longrightarrow \quad V_{12} = \vec{\dot{x}}_1^T \vec{\dot{x}}_{12} + \frac{1}{2}|\vec{\dot{x}}_{12}|^2 - \sum_k \int_{t_0}^{t} (\overline{F}_{2_k}\dot{x}_{2_k} - \overline{F}_{1_k}\dot{x}_{1_k})dt - \omega_e(x_{12_1}\dot{x}_{2_2} - x_{2_2}\dot{x}_{12_1} - x_{1_1}\vec{\dot{x}}_{12_2} + x_{12_2}x_{1_1}) - E_{0_{12}}$$

$$\int_{t_0}^{t} \frac{\partial V_{12}}{\partial t}dt = \int_{t_0}^{t} \frac{\partial V^E_{12}}{\partial t}dt + \cancel{\int_{t_0}^{t} \frac{\partial V^{TV}_{12}}{\partial t}dt} \approx \int_{t_0}^{t} \frac{\partial V^E_{12}}{\partial t}dt$$

The new proposed energy equation [Guo et. al., 2015]

$$V = V^E + V^{TV} = V^E + V_{TGP} + V_{ET} + V_{OT} + V_{TVOS}$$

$$\int_{t_0}^{t} \frac{\partial V_{12}}{\partial t}dt = \int_{t_0}^{t} \frac{\partial V^E_{12}}{\partial t}dt + \int_{t_0}^{t} \frac{\partial V^{TV}_{12}}{\partial t}dt = \int_{t_0}^{t} \frac{\partial V^E_{12}}{\partial t}dt + \left(\int_{t_0}^{t} \frac{\partial V^{TGP}_{12}}{\partial t}dt + \int_{t_0}^{t} \frac{\partial V^{ET}_{12}}{\partial t}dt + \int_{t_0}^{t} \frac{\partial V^{OT}_{12}}{\partial t}dt + \int_{t_0}^{t} \frac{\partial V^{TVOS}_{12}}{\partial t}dt\right)$$

$$V^E_{12} = \vec{\dot{x}}_1^T \vec{\dot{x}}_{12} - V^{TV}_{12} + \frac{1}{2}|\vec{\dot{x}}_{12}|^2 - \sum_k \int_{t_0}^{t} (\overline{F}_{2_k}\dot{x}_{2_k} - \overline{F}_{1_k}\dot{x}_{1_k})dt + \int_{t_0}^{t} \frac{\partial V^E_{12}}{\partial t}dt + \int_{t_0}^{t} \frac{\partial V^{TV}_{12}}{\partial t}dt - E_{0_{12}}$$

Figure 2: The detailed equation expression of the proposed potential rotational terms

- The processing steps and background force models considered in our approach using the EBA software of the study [Shang et al., 2015].

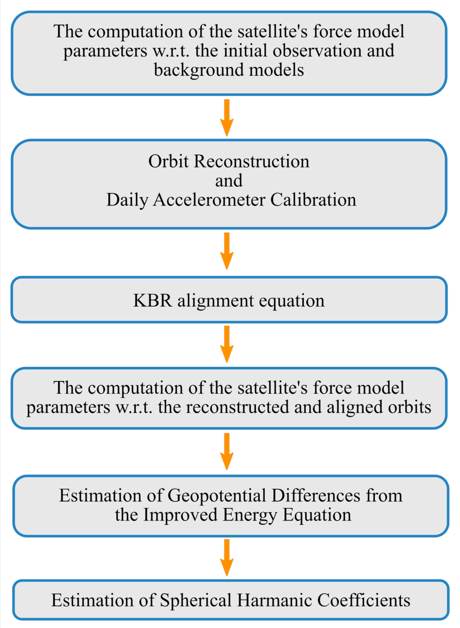

Model Description	
Static Field:	GGM05C (Ries et al., 2016)
Time-Variable Field:	EIGEN-6C (Förste et al., 2012)
Ocean Tides:	EOT11a (Savcenko and Bosch, 2012)
N-body Perturbation:	DE421 (Folkner et al., 2008)
Solid Earth Tides	
Pole Tides	
Ocean Pole Tides	IERS2010 (Petit and Luzum, 2010)
Relativistic Perturbations	
Atmospheric Tides:	(Biancale and Bode, 2006).
Input data	
GNV1B and ACC1B RL02	(Case et al., 2010)
KBR1B and SCA1B RL03	(GRACE, 2018)
AOD1B RL06	(Dobslaw et al., 2017)
Parametrization	
Degree and order: 60 × 60	
Orbit arc length : Daily	
ACC calibration :	The daily bias parameters (offset, linear and quadratic trends) are estimated foreach day. While XSRF direction of scale parameters are adjusted to 0.98 after 2010 and keep 1.0 before 2010. Other directionsare fixed by recommended scale parameters as in (Bettadpur, 2009).
KBR Empirical Parameters :	Bias, Bias rate and 1 cycle per revolutionas in (Liu, 2008)

(b)

Figure 3: (a): The descriptions of the processing steps and (b): used background models in our approach

B. Numerical Investigation

- B.1 Before Gravity Inversion
- The basic purpose of the KBR alignment equation, which is a novel equation of [Shang et al., 2015], is to replace the inter-satellite velocity pitch of orbit with that from KBR range-rate measurements by considering the geometric relationship between the orbit velocity vectors and the range rate measurements. Thus, the KBR range-rate data is used implicitly in the EBA equation via alignment equations avoiding adjustment or any approximation for usage range-rate data.

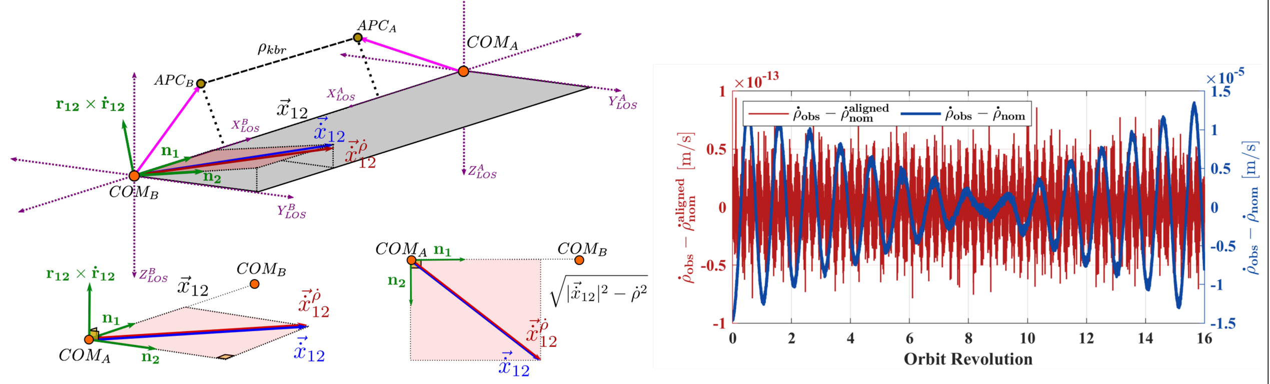

$$\vec{\dot{x}}^{\rho}_{12} = \dot{\rho}\frac{\vec{x}_{12}}{|\vec{x}_{12}|} + \sqrt{|\vec{\dot{x}}_{12}|^2 - \dot{\rho}^2}\,\frac{\vec{x}_{12} \times \vec{\dot{x}}_{12} \times \vec{x}_{12}}{|\vec{x}_{12} \times \vec{\dot{x}}_{12} \times \vec{x}_{12}|}$$

(a) (b)

Figure 4: (a): The geometric relationship between the orbit velocity vectors and the range rate measurements. (b): The differences between the observed and nominal range-rates before and after KBR alignment.

- The daily estimated geopotential is illustrated in Fig. 5. The estimated GPDs include systematic errors which appear as the so-called bow-tie pattern, which is sourced from the resonant effect of orbits. The main reasons for this effect are explained by the errors in the initial state of positions and velocities as well as the differences between the background force models and true models [Colombo, 1984, Liu, 2008]. In order to eliminate these effects, the kinematic empirical parameter fitting is applied to the differences between the observed and the nominal range, range-rate or range-accelerations [Kim, 2000, Liu, 2008]. Thus, residual range-rates can be used to calculate the gravity field models. In contrast to using the residual range rates, the residuals between the estimated GPDs and the fitted model, i.e. fitting the kinematic empirical parameters at the estimated GPD level, are calculated in our approach, since the aligned velocity components include these systematic errors and transplant to the estimated GPDs. Hence, the estimated GPDs are eliminated from the systematic effects.

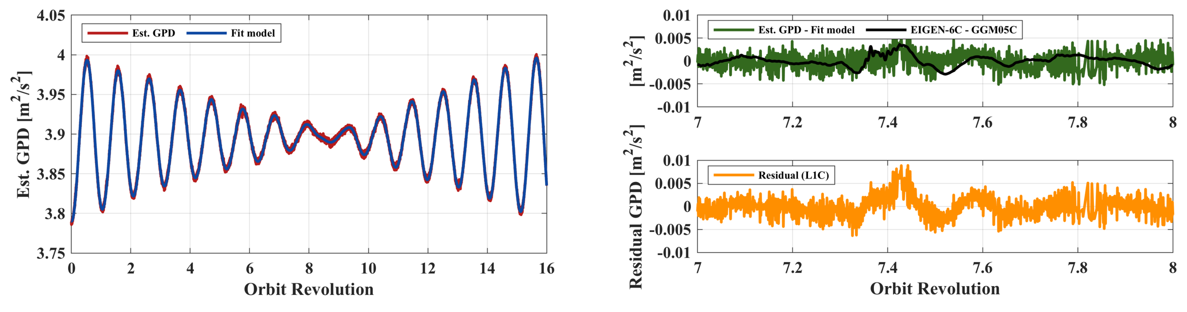

Figure 5: (a): The daily estimated GPDs from the energy equation using the reconstructed and aligned orbits for 2009-02-01, (b): The residuals in one full orbit revolution

- The Multiresolution Wavelet Decomposition (MWD) approach is used to understand the effects of the error and the noise sources of our models fragmenting into two subparts in sense of before and after gravity inversion. While the estimated GPD residuals are analyzed in the first part, the second part is based on calculating the insitu predicted GPDs at satellite altitudes from L1C model (the calculated models for this study) and CSR RL06 models and getting the differences of these predicted GPDs. For this purpose, the residuals are fragmented into three time-scale band considering the dominant frequency regions: the short-time scale (frequency > 12.5 mHz), the medium-time scale (3.125 mHz < frequency < 12.5 mHz) and the long-timescale (frequency < 3.125). The MWD is applied using discrete Daubechies wavelet transform considering 20 vanishing moments decomposing the residual signal into 8 discrete approximation and detail levels. These detail levels are grouped into three subbands w.r.t. time-scales bands as in the study of [Behzadpour et al., 2019].

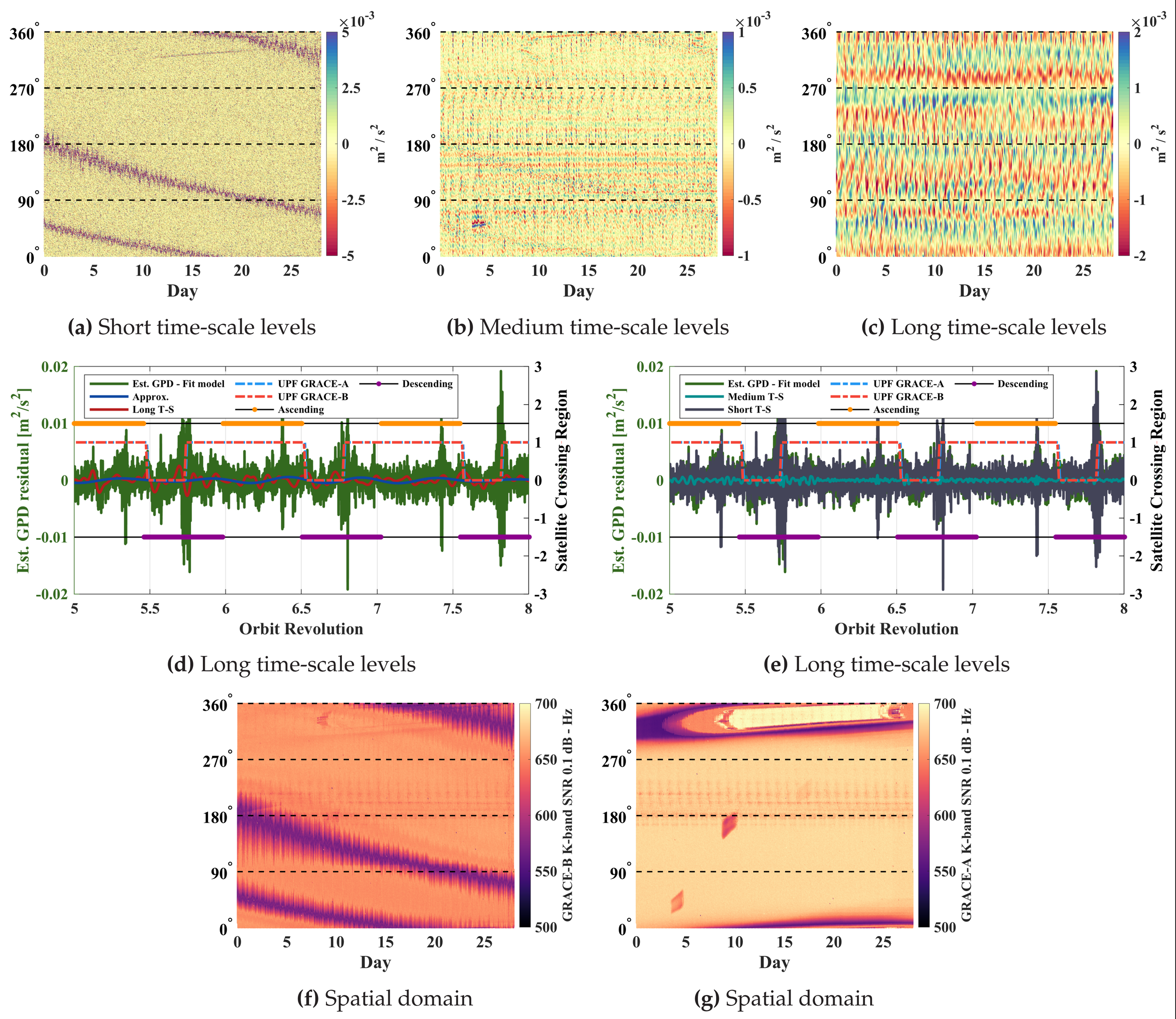

Figure 6: The L1C residuals MWD results in terms of relevant time-scales in February 2009

- According to Fig. 7a, 7b, 7c and 7d, the scattering plotting of L1C residuals are illustrated in terms of GRACE-A/B K/Ka-band SNR values along with the daily time series of the 01 February 2009. This type of comparison gives information about which band signal dominates the inter-satellite velocity components and L1C residuals. The white and red color dots represent the measurements or residuals below the minimum required SNR values w.r.t to different bands. Although all band noises affect the observables, the dominant noise source is stemmed from GRACE-B K-band which is related to the temperature changes of the satellite as in Fig 7c. While the GRACE-B Ka-band SNRs vary randomly from 2004 to 2011, the other band SNRs vary periodically. The GRACE-B Ka-band is not considered in the data processing [Goswami et al., 2018]. This band noises are stimulated to whole time-series of observables with low-level SNRs. The detailed investigation of the high-frequency noise sources is explained by the study of [Harvey et al., 2017, Goswami et al., 2018].

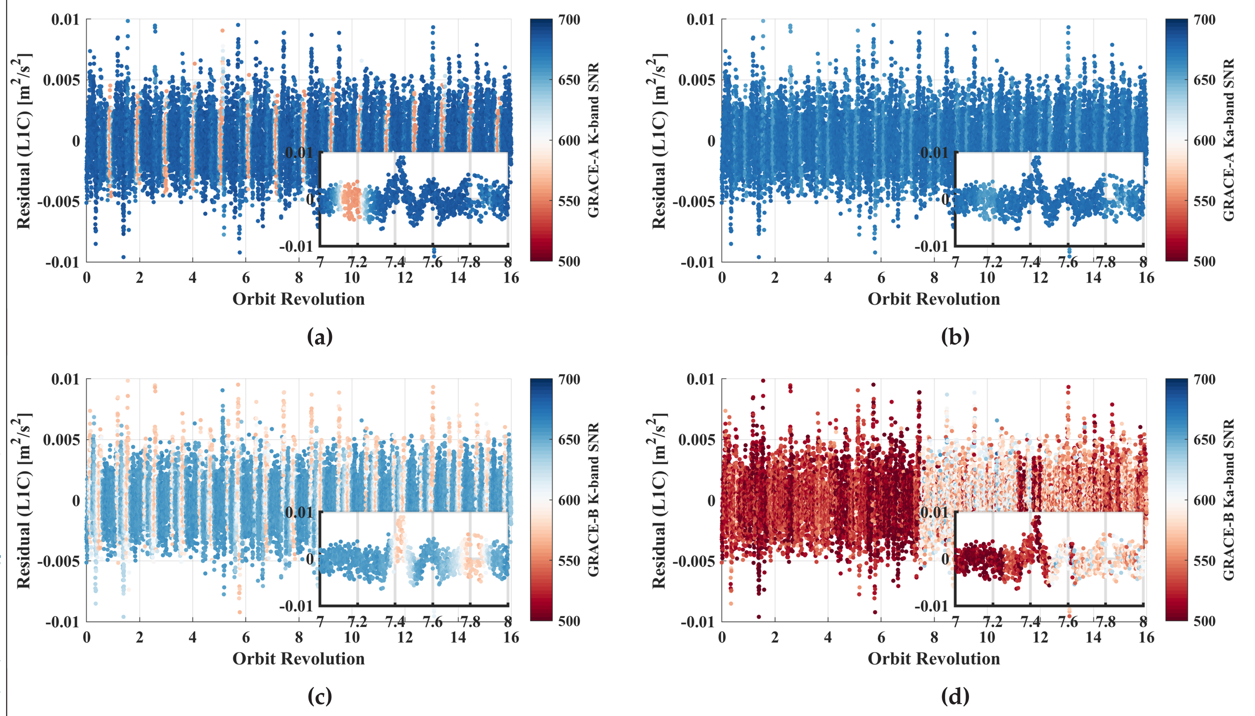

Figure 7: The daily time series of L1C residuals in terms of the scattering of the GRACE-A/-B K/Ka-band SNR only for 01 February 2009

- B.2 After Gravity Inversion

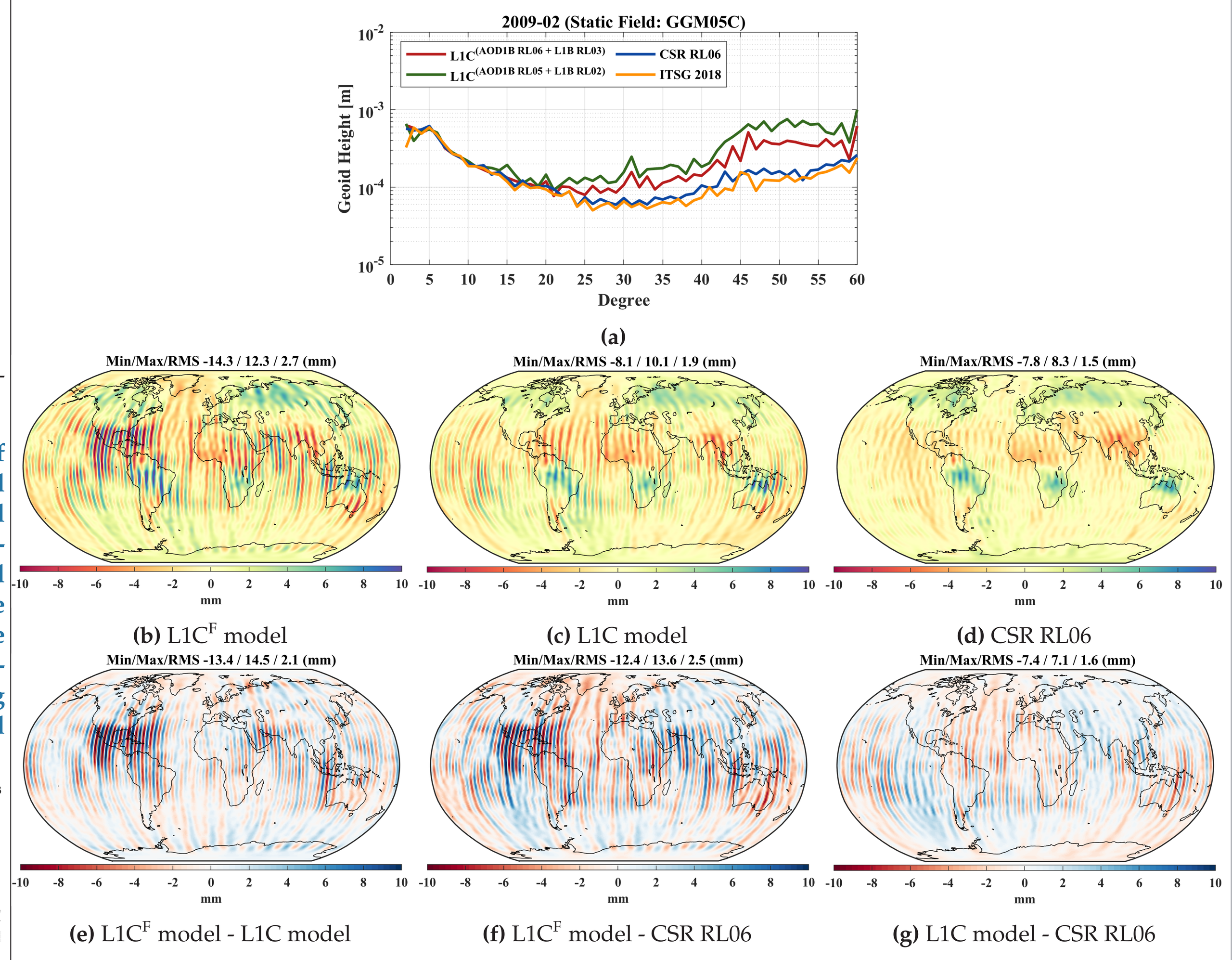

Figure 8: (a): Degree variances of the models in terms of the geoid undulation without applying any filtering to SHCs for February 2009, the spatial illustrations of (b): L1C[F] model (calculated using the AOD1B RL05 + L1B RL02), (c): L1C model (calculated using the AOD1B RL06 + L1B RL03) and (d): CSR RL06. In addition, (d), (e) and (f): The differences of model undulations using the same monthly models

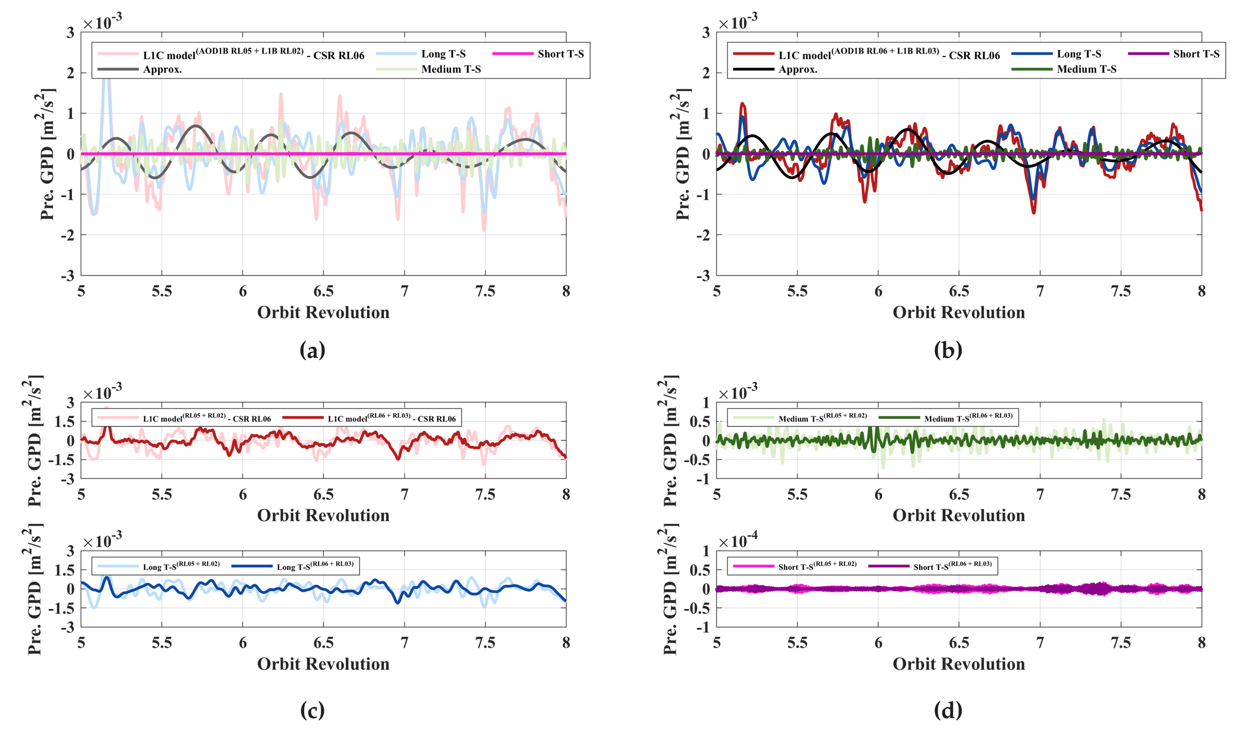

Figure 9: MWD results of the predicted GPD differences between the L1C model and CSR RL06, and between L1C[F] model - CSR RL06 at satellite altitudes.

C. Discussion and Conclusion

- Our temporal gravity field solutions have comparable accuracy with CSR RL06 and ITSG-Grace2018 for low degrees up to d/o 20 but less accurate for high degrees. In addition, the estimated SHCs are highly correlated. This high correlation is stemmed from the low-frequency noise, i.e. the orbital resonance directly affects the SHC estimates.
- To use the range-rate observation avoiding any adjustment or approximation, the KBR alignment equation is used to calculate inter-satellite velocity differences. This equation enables the use of range-rate data directly in the energy equation. However, the alignment process while intend to take the advantage of high-precision range-rate observations, it also introduces the systematic errors due to the relationship between the orbit and range-rates in the alignment equation.
- The kinematic empirical parameter is fitted and removed from the estimated GPDs. But there is still effect of these systematic errors in our estimated SHCs, i.e. the resonant effect dominates and reduces the model accuracy. In other words, it can be evaluated that the removal of the empirical parameters at the estimated GPDs level is not sufficient and more rigorous work is required.
- On the other hand, the background models are evaluated two times in our processing chain: first, the accelerations are calculated in orbit determination, second, the potentials using the background models are also calculated in energy equations. This implementation might be increasing the systematic effect of orbit resonance.
- MWD results of L1C residual and the predicted GPDs of models show that the main contributor to lower model accuracy is the low-frequency noises. The handling of antenna offset correction is also important to increase model accuracy. The high-frequency noise of L1C residuals is especially correlated with the signal quality of GRACE-B K-band.
- To remove the low-frequency noise and increase our model accuracy, the empirical parameters can be co-estimated during the gravity inversion considering the quasi-periodic characterization of the differences between the predicted GPDs of ITU and CSR RL06 models in terms of the dominant periods.
- The antenna offset corrections of KBR observations are calculated w.r.t. the reconstructed orbits to reduce the medium time-scale subband errors. In contrast to eliminating the high-frequency noise in L1C residuals, the frequency-dependent, i.e. considering the high-frequency subband of L1C in the results of the MWD approach, correlations of residuals can be used to as a stochastic model of gravity inversions.
- As a result, the lower model accuracy of estimated temporal gravity field models from improved energy balance model approach is depends on both low - and high - frequency in our temporal gravity solutions. Especially the background model uncertainties are the dominant error sources in our temporal gravity solutions.

D. References

[Behzadpour et al., 2019] Behzadpour, S., Mayer-Gürr, T., Flury, J., Klinger, B., and Goswami, S. (2019). Multiresolution wavelet analysis applied to grace range-rate residuals. *Geoscientific Instrumentation, Methods and Data Systems*, 8(2):197–207.

[Bettadpur, 2018] Bettadpur, S. (2018). Gravity recovery and climate experiment utcsr level-2 processing standards document. Technical report, University of Texas at Austin.

[Biancale and Bode, 2006] Biancale, R. and Bode, A. (2006). Mean annual and seasonal atmospheric tide models based on 3-hourly and 6-hourly ECMWF surface pressure data. Scientific technical report str, Deutsches GeoForschungsZentrum, Potsdam.

[Case et al., 2010] Case, K., Kruizinga, G., and Wu, S.-C. (2010). Grace level 1b data product user handbook. Technical report. JPL Publication D-22027.

[Colombo, 1984] Colombo, O. L. (1984). *The global mapping of gravity with two satellites*. Rijkscommissie voor Geodesie.

[Dobslaw et al., 2017] Dobslaw, H., Bergmann-Wolf, I., Dill, R., Poropat, L., Thomas, M., Dahle, C., Esselborn, S., König, R., and Flechtner, F. (2017). A new high-resolution model of non-tidal atmosphere and ocean mass variability for de-aliasing of satellite gravity observations: AOD1B RL06. *Geophysical Journal International*, 211(1):263–269.

[Folkner et al., 2008] Folkner, W. M., Williams, J. G., and Boggs, D. H. (2008). The planetary and lunar ephemeris de 421. *JPL IOM 343R-08-003*.

[Förste et al., 2012] Förste, C., Bruinsma, S., Shako, R., Abrikosov, O., Flechtner, F., Marty, J.-C., Lemoine, J.-M., Dahle, C., Neumeyer, H., Barthelmes, F., et al. (2012). A new release of eigen-6: The latest combined global gravity field model including lageos, grace and goce data from the collaboration of gfz potsdam and grgs toulouse. In *EGU General Assembly Conference Abstracts*, volume 14, page 2821.

[Goswami et al., 2018] Goswami, S., Devaraju, B., Weigelt, M., and Mayer-Gürr, T. (2018). Analysis of grace range-rate residuals with focus on kbr instrument system noise. *Advances in Space Research*, 62(2):304 – 316.

[GRACE,] GRACE. Grace level 1b jpl release 3.0 ver. 3. po.daac ca usa.

[Guo et al., 2015] Guo, J. Y., Shang, K., Jekeli, C., and Shum, C. K. (2015). On the energy integral formulation of gravitational potential differences from satellite-to-satellite tracking. *Celestial Mechanics and Dynamical Astronomy*, 121(4):415–429.

[Harvey et al., 2017] Harvey, N., Dunn, C. E., Kruizinga, G. L., and Young, L. E. (2017). Triggering conditions for grace ranging measurement signal-to-noise ratio dips. *Journal of Spacecraft and Rockets*, 54(1):327–330.

[Kim, 2000] Kim, J. (2000). *Simulation study of a low-low satellite-to-satellite tracking mission*. PhD thesis, Citeseer.

[Kvas et al., 2019] Kvas, A., Behzadpour, S., Ellmer, M., Klinger, B., Strasser, S., Zehentner, N., and Mayer-Gürr, T. (2019). Itsg-grace2018: Overview and evaluation of a new grace-only gravity field time series. *Journal of Geophysical Research: Solid Earth*, 124(8):9332–9344.

[Liu, 2008] Liu, X. (2008). Global gravity field recovery from satellite-to-satellite tracking data with the acceleration approach.

[Mayer-Gürr et al., 2018] Mayer-Gürr, T., Behzadpour, S., Kvas, A., Ellmer, M., Klinger, B., Strasser, S., and Zehentner, N. (2018). Itsg-grace2018: Monthly, daily and static gravity field solutions from grace.

[Petit and Luzum, 2010] Petit, G. and Luzum, B. (2010). Iers conventions (2010). Technical report, BUREAU INTERNATIONAL DES POIDS ET MESURES SEVRES (FRANCE).

[Ries et al., 2016] Ries, J., Bettadpur, S., Eanes, R., Kang, Z., Ko, U., McCullough, C., Nagel, P., Pie, N., Poole, S., Richter, T., et al. (2016). The combined gravity model ggm05c. *GFZ Data Services*.

[Savcenko and Bosch, 2012] Savcenko, R. and Bosch, W. (2012). Eot11a - empirical ocean tide model from multi-mission satellite altimetry.

[Shang et al., 2015] Shang, K., Guo, J., Shum, C., Dai, C., and Luo, J. (2015). GRACE time-variable gravity field recovery using an improved energy balance approach. *Geophysical Journal International*, 203(3):1773–1786.

E. Acknowledgement

- We would like to thank the German Academic Exchange Service (DAAD - Deutscher Akademischer Austauschdienst) for funding to one-year research grant.